AAAS
Ultrafast Science
Volume 2022, Article ID 9894358, 8 pages
https://doi.org/10.34133/2022/9894358

Ultrafast Science
A SCIENCE PARTNER JOURNAL

Research Article

13.4 fs, 0.1 Hz OPCPA Front End for the 100 PW-Class Laser Facility

Xinliang Wang,[1] Xingyan Liu,[1] Xiaoming Lu,[1] Junchi Chen,[1] Yingbin Long,[1] Wenkai Li,[1] Haidong Chen,[1,2] Xun Chen,[1,2] Peile Bai,[1,2] Yanyan Li,[1] Yujie Peng,[1] Yanqi Liu,[1] Fenxiang Wu,[1] Cheng Wang,[1] Zhaoyang Li,[3] Yi Xu,[1] Xiaoyan Liang,[1] Yuxin Leng,[1,2] and Ruxin Li[1]

[1]*State Key Laboratory of High Field Laser Physics and CAS Center for Excellence in Ultra-intense Laser Science, Shanghai Institute of Optics and Fine Mechanics (SIOM), Chinese Academy of Sciences (CAS), Shanghai 201800, China*
[2]*Center of Materials Science and Optoelectronics Engineering, University of Chinese Academy of Sciences, Beijing 100049, China*
[3]*Zhangjiang Laboratory, Shanghai 201210, China*

Correspondence should be addressed to Xiaoming Lu; xiaominglu@siom.ac.cn, Yi Xu; xuyi@siom.ac.cn, and Yuxin Leng; lengyuxin@siom.ac.cn

Received 14 March 2022; Accepted 27 May 2022; Published 18 June 2022

Here, we report the recent progress on the front end developed for the 100 PW-class laser facility. Using 3 stages of optical parametric chirped-pulse amplification (OPCPA) based on lithium triborate (LBO) crystals, we realized a 5.26 J/0.1 Hz amplified output with a bandwidth over 200 nm near the center wavelength of 925 nm. After the compressor, we obtained a pulse duration of 13.4 fs. As the compression efficiency reached 67%, this OPCPA front end could potentially support a peak power of 263 TW at a repetition rate of 0.1 Hz. To the best of our knowledge, among all the 100 TW-level OPCPA systems, it shows the widest spectral width, the shortest pulse duration, and it is also the first OPCPA system working at a repetition-rate mode.

1. Introduction

The invention of chirped-pulse amplification (CPA) technique [1] has significantly promoted the development of high-intensity femtosecond laser systems. The peak power of femtosecond laser has been raised from terawatt (TW) level to petawatt (PW) level during the past decades. In recent years, multi-PW and 10 PW-class laser facilities have been constructed by many laboratories around the world, such as CoReLS 4.2 PW laser [2], SULF-10 PW laser [3], and ELI-10 PW laser [4]. However, limited by the available crystal size [5] and the inherent transverse parasitic lasing effect [6, 7] in the Ti: sapphire crystal, it is not easy to directly boost the peak power to a higher level by using the CPA scheme.

Alternatively, optical parametric chirped-pulse amplification (OPCPA) [8] is an another scheme to achieve super-intense femtosecond laser. So far, the highest output based on OPCPA is 4.9 PW of the CAEP-PW laser facility, which works at the center wavelength of 800 nm [9]. Near 900 nm central wavelength, many nonlinear crystals, such as lithium triborate (LBO) and deuterated potassium dihydrogen phosphate (DKDP), can realize over 200 nm bandwidth when pumped with high-energy frequency-doubled Nd:YAG or Nd:glass lasers. Especially, the existing crystal growth technologies can support large DKDP crystals over 400 mm size [10]. Therefore, the DKDP-based OPCPA scheme is considered a promising approach for developing 100 PW-class laser facilities. The Vulcan 10 PW project at the Rutherford Appleton Laboratory was designed to generate pulses with energies greater than 300 J and with durations less than 30 fs at a central wavelength of 910 nm [11]. The EP OPAL project at the University of Rochester was aimed at building a 75 PW laser by using DKDP crystal centered at 910 nm [12]. At present, the technology development platform of the EP OPAL facility has realized a single-shot 21.5 fs/

350 TW output by using 70% deuterated DKDP crystals [13]. Osaka University also demonstrated the conceptual design of the Gekko-EXA which would aim to obtain 50 PW output [14]. Recently, Institute of Applied Physics proposed the XCELS (eXawatt Center for Extreme Light Studies) project, which aims to build 12 channels of 15 PW beam and use coherent addition for laser-target interaction [15]. As the front end for XCELS-Proto, a peak power of 560 TW had been realized by using 3 stages of parametric amplification based on DKDP crystals in 2007, with a compressed pulse duration of 43 fs [16]. To date, the reported 100 TW or PW-level OPCPA laser systems all work in the single-shot mode and the pulse durations are around or above 20 fs.

In 2018, the project of Shanghai X-ray Free Electron Laser (SHINE) was launched. An important part of this project is the Station of Extreme Light (SEL), in which the powerful light of the 100 PW-class laser (SEL-100 PW) will combine with the X-ray free laser (XFEL) for the researches on strong-field QED physics [17, 18]. In this project, an OPCPA 100 PW laser facility will be developed, which can provide the focused intensity of more than 10^{23} W/cm^2 [19, 20]. The SEL-100 PW laser mainly includes an OPCPA front end working at a repetition rate of 0.1 Hz, two-stage DKDP-based main amplifiers pumped by a 10 kJ-level Nd:glass laser, and a final optic assembly which can recompress the amplified laser to sub-15 fs pulse width and realize 100 PW-level peak power. The OPCPA front end plays an important role in the SEL-100 PW facility, which will not only provide high-performance seed pulses for the subsequent amplifiers but also be used as a test platform for some key components and technologies.

In the present study, we demonstrated the performances of the 0.1 Hz OPCPA front end for the SEL-100 PW laser facility. By seeding a broadband pulse, we realized 210 nm broadband amplification at the central wavelength of 925 nm using three-stage LBO-based OPCPA amplifiers. The energy of the seed pulse was boosted to 5.26 J. After a two-grating compressor, the pulse duration was measured to be 13.4 fs. With the compression efficiency of 67%, a peak power of 263 TW could potentially be achieved. To the best of our knowledge, among all the reported 100 TW-level OPCPA systems, it shows the widest spectral width, the shortest pulse duration, and it is also the first OPCPA system working at a repetition-rate mode.

2. Materials and Methods

A schematic of the front end for SEL facility is shown in Figure 1. It consists of a high contrast ultrabroadband seed, a double-grating Offner stretcher, three stages of OPCPA amplifiers (OPCPA-1/-2/-3) and the corresponding pump lasers (Pump-1/-2/-3), and a pulse compressor. The front end was designed to support a 0.1 Hz amplified output with the energy above 5 J and the spectral width of >200 nm, which could support a 200 TW-level peak power if the pulse could be compressed below 15 fs. To achieve the designed output parameters, the main challenges include the ultrabroadband amplification beyond 200 nm spectral width with long-pulse (~4 ns) pumping laser and ultrabroadband dispersion compensation of large-chirped pulses to obtain sub-15 fs compressed pulse duration. Additionally, Pump-3, which can output 25 J of 527 nm pump energy at the repetition rate of 0.1 Hz, is also the key factor to support our front end working at a repetition-rate mode.

For ultrabroadband dispersion compensation, in our previous work, we had demonstrated that the compressed pulse duration near Fourier transform limit (FTL) could be obtained in an OPCPA systems by using the double-grating Offner stretcher even without any extra precise dispersion compensation [21]. Thanks to the real aberration-free characteristic, it endows of the double-grating Offner stretcher with the advantage of perfect-dispersion-match with conjugated Treacy compressor, which could significantly facilitate the dispersion management in an OPCPA system featuring a small amount of material dispersion.

To obtain a broadband optical parametric amplification, the noncollinear phase-matching scheme was considered. Beta barium borate (BBO), LBO, and DKDP are commonly used crystals to realize the broadband amplification. The main parameters for noncollinear OPCPA based on three crystals are listed in Table 1, considering that the pump intensity is 1 GW/cm^2 and the small signal gain of ~200. The gain bandwidths of three crystals at 925 nm phase-matching signal wavelength are shown in Figure 2 by solving the coupled wave equations that describe the nonlinear amplification process. Compared with BBO and DKDP ($D = 80\%$), LBO features the moderate nonlinear coefficient (0.79 pm/V), the availability of large size at tens of millimeters [22, 23], the smallest walk-off angle (0.47 deg), and the broadband gain spectrum (202 nm, full width at half maximum, FWHM) around 925 nm central wavelength. These features make LBO the excellent nonlinear gain medium for OPCPA. Additionally, the LBO crystal supports a better overlap of the gain spectrum with DKDP ($D = 80\%$) crystal, which guarantees that the spectral region of the front end can match the gain region of the following main DKDP amplifiers.

In order to improve the performance of this laser system, several technical measures were taken. Firstly, a beam pointing-locking setup (Aligna 4D, TEM Messtechnik) was installed after the pulse stretcher to improve the beam pointing stability, which can alleviate the impact on efficiency and bandwidth of the OPCPA induced by the beam pointing fluctuation. With Aligna 4D, the standard deviation of pointing fluctuation in horizontal and vertical directions was measured to be 1.95 μrad and 2.61 μrad, respectively. Secondly, to minimize the effect of temperature drift, three crystal ovens with control accuracy of ±0.05°C were used in three OPCPA amplifiers. The seed pulses of the three pump lasers were generated by the single longitudinal mode fiber sources, which were integrated with an arbitrary waveform generator (ModBox-IQ, IXBLUE) for obtaining the super-Gaussian temporal shape. The spatial profile of all the three pump beams was also shaped as high-order super-Gaussians. After the regenerative amplifiers of three pump lasers, the beam was preliminarily shaped into super-Gaussians shape by using a beam shaper, which

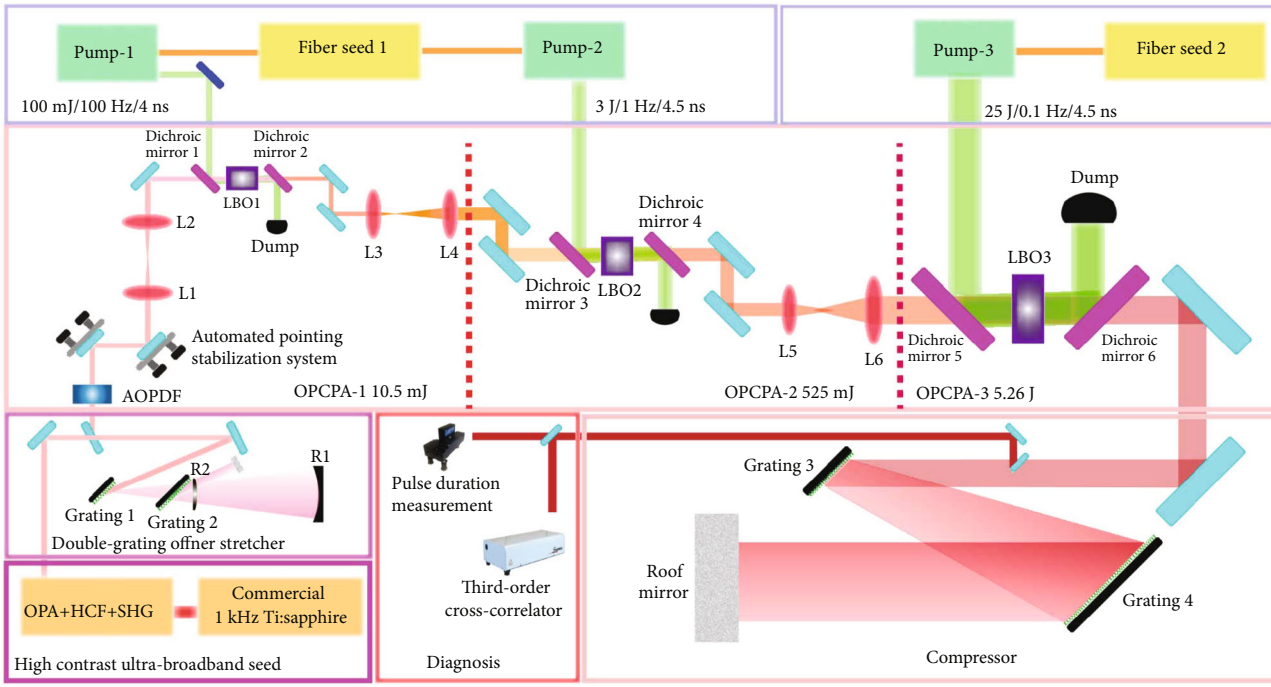

Figure 1: Schematic of the 263 TW/0.1 Hz OPCPA front end. AOPDF: Acoustooptic programmable dispersive filter; HCF: Hollow core fiber; OPA: Optical parametric amplification; SHG: Second harmonic generation.

Table 1: Parameters of the noncollinear optical parametric chirped-pulse amplification for BBO, LBO, and DKDP ($D = 80\%$) crystals.

Parameters	LBO	BBO	DKDP (80%)
(θ, φ)	(90°,13.78°)	(23.56°,0°)	(37.68°,45°)
α	1.37°	2.25°	0.61°
ρ	0.47°	3.27°	1.48°
d_{eff}(pm/V)	0.79	2.02	0.24

Here, (θ, φ), α, and ρ are phase-matching angle, noncollinear angle, and walk-off angle, respectively.

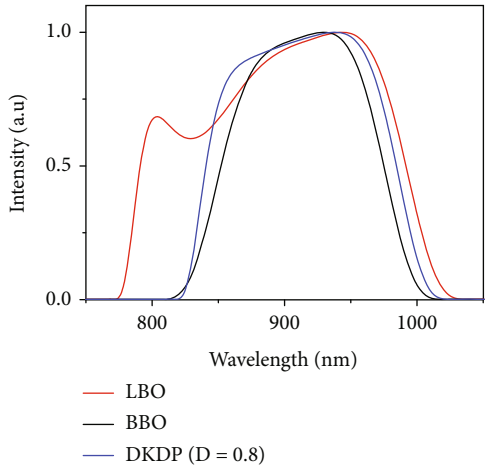

Figure 2: Gain spectra of BBO, LBO, and DKDP ($D = 80\%$) crystals with the pump intensity of 1 GW/cm^2 and the small signal peak gain of ~200.

consisted of a beam expander and a serrated aperture. In the following amplifier chains, the geometry of the pumping chamber, the flow of the cooling water, the doping-concentration, and the dimensions of the laser rods were optimized to further improve beam quality. Finally, the signal and pump pulses were electronically synchronized using a master clock circuit (Master Clock, Thales Laser), which featured a typical jitter of less than 50 ps.

3. Results and Discussion

To obtain an ultrabroadband and high-contrast seed source, there are two available technical approaches. The first one is just based on the midinfrared optical parametric amplification (OPA) and femtosecond second harmonic generation (SHG) [24]. The other one is the combination of midinfrared OPA, hollow-core fiber (HCF), and femtosecond SHG [25], which was adopted in this work. Pumped by a commercial 1 kHz Ti: sapphire amplifier (Astrella, Coherent), the midinfrared OPA can generate an energy of 750 μJ around 1850 nm central wavelength with a pump energy of 7.2 mJ. The OPA process realized wavelength shift from 800 nm to 1850 nm and amplification of the 1850 nm pulse, which also preliminary improved the temporal contrast. The following HCF setup could further broaden the spectrum and optimize the beam quality of the OPA output. Finally, the pulses were frequency doubled by using a BBO crystal to obtain seed pulses with an energy of ~100 μJ and full spectral width of 265 nm near the center wavelength of 925 nm, as shown in Figure 3. The final SHG process further improved the temporal contrast of the pulses.

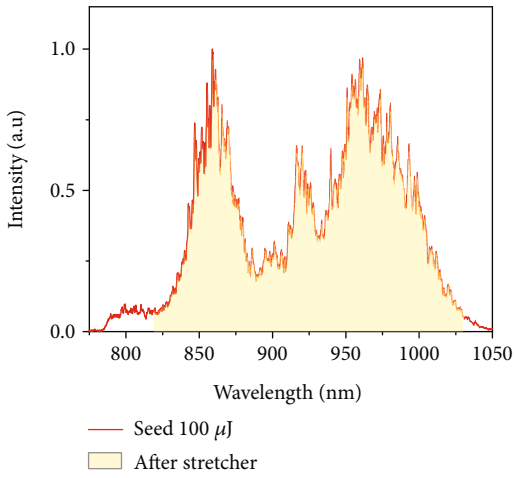

FIGURE 3: Spectrum of the seed pulse (red line) and the bandwidth of the stretcher (yellow shadow).

The seed pulses were injected into a double-grating Offner stretcher. The stretcher included a concave mirror (R1 = −2000 mm), a convex mirror (R2 = 1000 mm), a roof mirror, and two 1480 lines/mm golden gratings (HORIBA). The angle of incidence (AOI) was about 62 deg, and the grating pair separation along the optical axis of the stretcher was 0.79 m. The stretcher supported a 210 nm bandwidth as shown in Figure 3 (yellow shadow), which covers 79.2% of the spectral region of the input pulses. To avoid energy loss, the pulses traveled only one round trip in the stretcher, corresponding to a total transmission efficiency of 53%. The chirped ratio of stretched pulses was 14.2 ps/nm. Considering the bandwidth of 210 nm, the stretched pulse duration was about 3 ns at the full width. After the pulse stretcher, a broadband acoustooptic programmable dispersive filter (AOPDF, HR45-650-1100) was used between the stretcher and the first OPCPA stage. The AOPDF, with a transmission efficiency of ~55%, is intentionally used for compensating the high-order dispersion in the upcoming 100 PW-class laser, rather than for the OPCPA front end.

For injection into the first OPCPA stage, the signal beam was downcollimated to 1.5 mm in diameter and imaged to the first LBO crystal, which is 10 mm × 10 mm × 30 mm in size and coated with antireflection films on both sides. The LBO crystal worked in the XOY plane. The phase-matching angle and the inner non-collinear angle were (90, 13.78) deg and 1.37 deg, respectively. The seed pulses of Pump-1 were amplified to an energy of 150 mJ by a LD pumped Nd:YAG regenerative amplifier and a LD-pumped double-pass Nd:YAG amplifier at 100 Hz repetition rate. After SHG, pump pulses with an energy of 100 mJ and a pulse duration of 4 ns were obtained. The pump beam was downcollimated to 2.1 mm in diameter and relay-imaged to the first LBO crystal. In order to obtain a broad spectral gain bandwidth and high conversion efficiency, the phase-matching angle, noncollinear angle, and the overlap area of the pump and the signal were carefully optimized. Finally, the signal pulse was amplified to 10.5 mJ. The spectrum of the OPCPA-1 output is shown in Figure 4(a). The spectrum covers a range of 820-1030 nm, which is limited by the bandwidth of the double-grating stretcher.

After OPCPA-1, the signal beam was upcollimated to 10 mm in diameter and relay-imaged to the second LBO crystal from the first LBO crystal in OPCPA-1. The crystal was 20 mm × 20 mm × 23 mm in size. The pump laser (Pump-2) for OPCPA-2 shared the same fiber source with Pump-1 and was mainly consisted of a LD-pumped Nd:YAG regenerative amplifier, a double-pass amplifier with two lamp-pumped Nd:YAG (φ16 mm) modules, a single-pass amplifier with two lamp-pumped Nd:YAG (φ21 mm) modules, and a SHG module. The output of Pump-2 could reach 3.5 J/4.5 ns/532 nm at a repetition of 1 Hz. The pump beam was downcollimated to 9 mm in diameter and relay-imaged to the second LBO crystal. With the pump energy of 2.8 J, the signal energy was amplified to 525 mJ, corresponding to a conversion efficiency of 18.6%. The spectrum and the near-field profile of the amplified pulse of OPCPA-2 are shown in Figures 4(a) and 4(d), respectively. Thanks to the flat-top beam profile of Pump-2 (Figure 4(b)), the amplified beam showed the super-Gaussian spatial profile.

The pump laser (Pump-3) for OPCPA-3 used a 1053 nm fiber source, as shown in Figure 1. In the preamplifiers, a LD-pumped Nd:YLF regenerative amplifier and a single-pass amplifier with two lamp-pumped Nd:YLF modules were used. After the preamplifiers, pump pulse was split into two beams and amplified by two double-pass main amplifiers, respectively. Here, we used Nd:glass as the gain medium in the main amplifiers because of its large size. Each main amplifier consisted of two lamp-pumped Nd:glass (φ25 mm) modules, which could enhance the energy to 18 J at 1053 nm wavelength. The two laser beams were combined by using a thin film polarizer and injected into an LBO-based type-II SHG module. The final output of Pump-3 could reach 25 J/527 nm at a repetition of 0.1 Hz. The pulse-to-pulse energy stability of Pump-3 laser was measured to be 2.1% in RMS. We also optimized the design of Nd:glass main amplifiers to make them work at a repetition rate of 0.1 Hz. The dynamic evolution process under the given xenon lamp parameters and the distribution of the temperature field inside the Nd:glass rods were numerically simulated. Based on the thermal analysis, effective cooling performances of large-diameter Nd:glass rods were realized by optimizing the design of pump-condensing cavity and the setting of water flow. Therefore, Pump-3 supported the repetition-rate mode of the final OPCPA stage.

Before the final OPCPA stage, the signal beam was upcollimated to 29 mm in diameter. The third LBO crystal for OPCPA-3 was 50 mm × 50 mm × 18 mm in size. At the pump energy of 22.5 J, the average output energy was 5.26 J, corresponding to the energy conversion efficiency of 21%. We measured the energy of consecutive 90 shots, and the RMS energy fluctuation was 2.4% (Figure 5(b)). The curve of output energy as a function of pump energy is shown in Figure 5(a), corresponding to a slope efficiency of 26.5%. The near-field beam profile of the amplified pulse shows some ring structures (Figure 4(e)), which comes from Pump-3 beam (Figure 4(c)). In the next step, we would further improve the near-field beam quality by using the far-

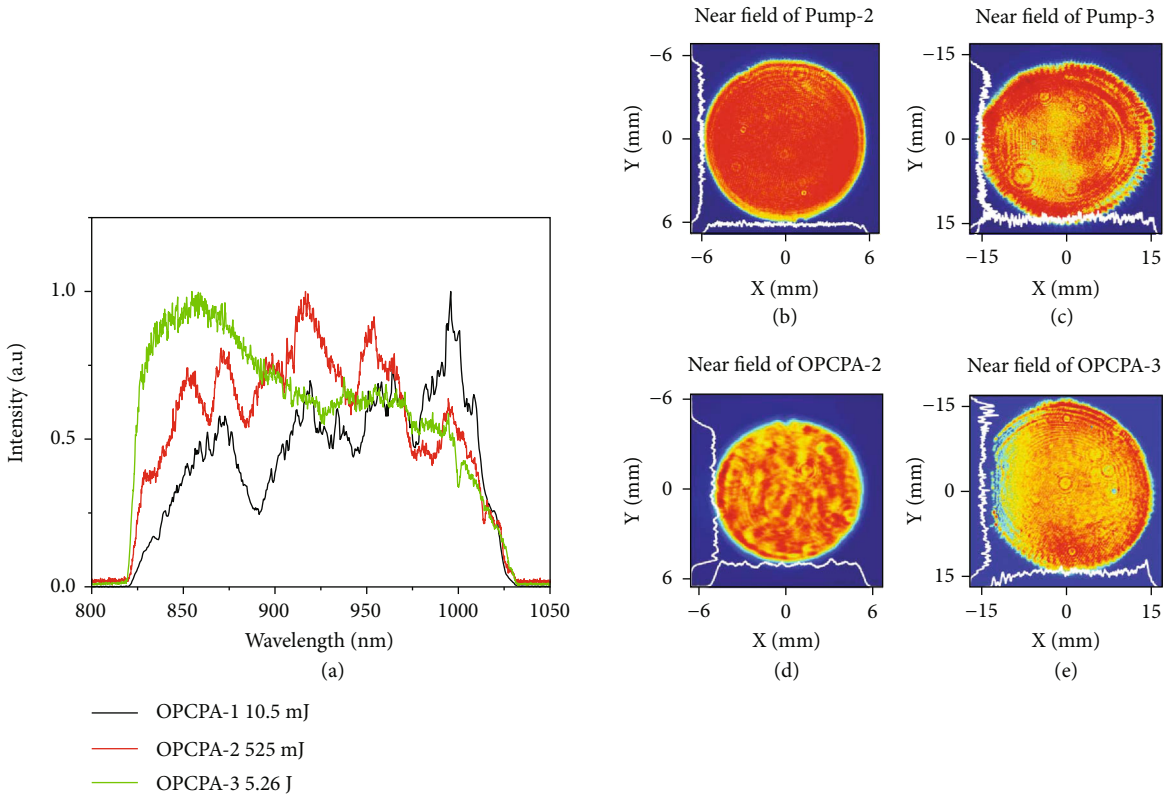

Figure 4: Spectra of the signals and beam profiles of the pumps and signals. (a) Output spectra of three OPCPA stages. (b) The near field beam profile of Pump-2. (c) The near field profile of Pump-3. (d) The near field profile of the amplified OPCPA-2. (e) The near field profile of the amplified OPCPA-3.

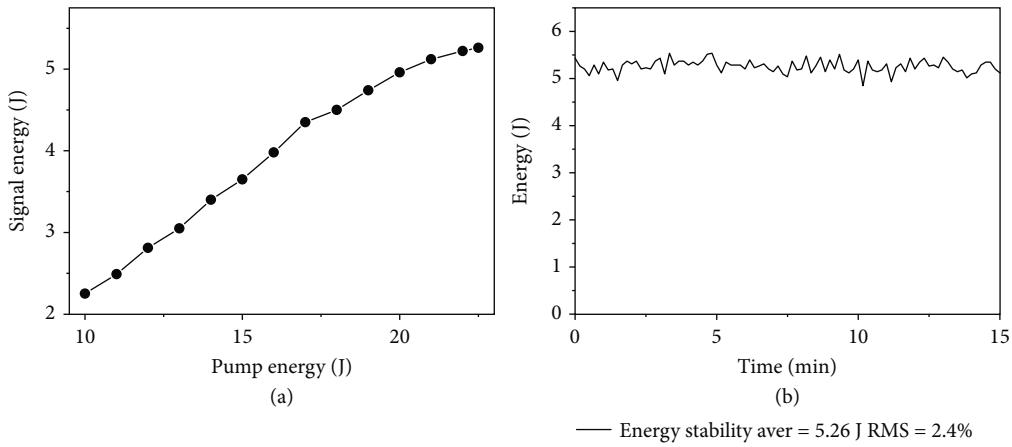

Figure 5: Output energy curve under different pump energies and energy stability of OPCPA-3. (a) Output energy as a function of pump energy. (b) Energy stability of OPCPA-3.

field filtering in the relay imaging system of Pump-3 laser. The spectrum of the output is shown in Figure 4(a). Here, the spectral modulation of the seed pulse was mitigated because of the saturation effect in OPCPA-3. The spectrum of the amplified pulse covered 210 nm at the full width, supporting the FTL pulse duration of 12.8 fs. To our knowledge, such ultrabroadband amplified spectrum using LBO crystal is firstly reported for the nanosecond OPCPA process with Joule-level pulse energy.

After OPCPA-3, the amplified pulses were sampled and injected into the compressor, which was consisted of two 1480 lines/mm gratings (HORIBA) and a roof mirror. The sizes of the two gratings are 420 (W) mm × 265 (H) mm and 565 (W) mm × 365 (H) mm, respectively. The designed diffraction efficiency of the gratings is ~94% for wavelength between 925 ± 100 nm at an AOI of 62 deg. The measured efficiency of the grating was as high as 92.3%. The roof mirror is 280 mm × 140 mm × 30 mm in size and coated with

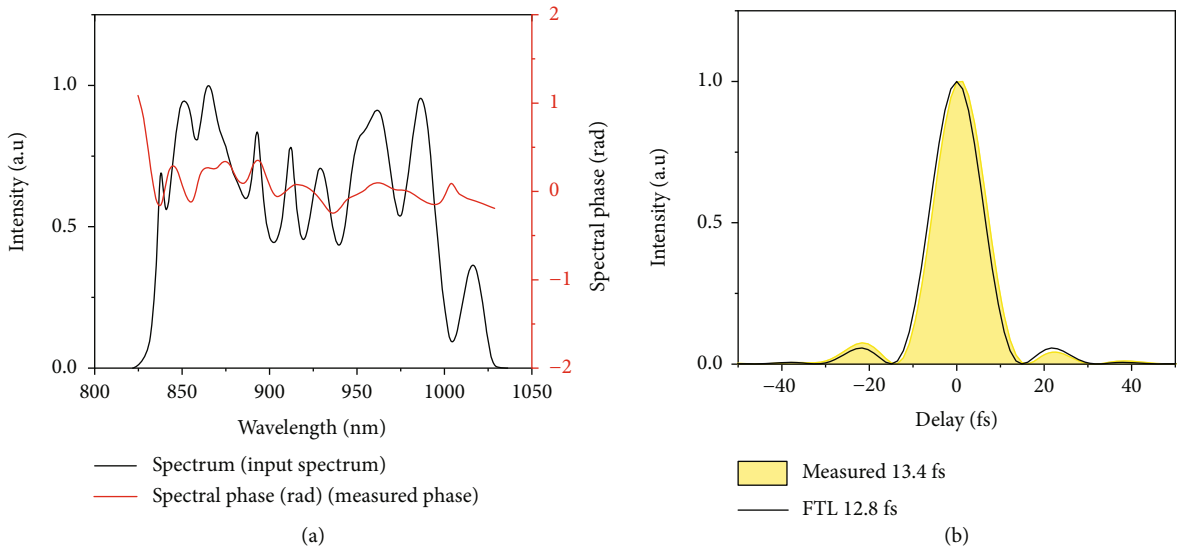

Figure 6: Characterization of compressed pulse. (a) Measured spectrum (black) and phase (red) of the 925 nm laser pulse. (b) Measured (yellow filled) and FTL (Fourier transform–limited, black solid) pulse duration of the compressed laser pulse.

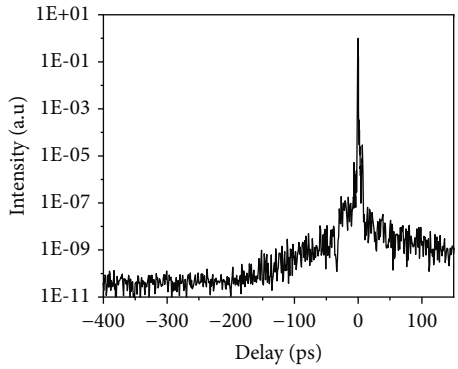

Figure 7: Third-order correlation measurement of the compressed pulse.

high-reflection film for a central wavelength of 925 nm (AOI is 45 deg). The spectral phase and temporal profile of the compressed pulses were measured by a Wizzler (USP4, Fastlite). Without any extra dispersion compensation, the pulse was well compressed by optimizing the distance and the angle of the grating pairs in the compressor. A typical pulse duration is 13.4 fs as shown in Figure 6(b), which is close to the FTL pulse duration. As shown in Figure 6(a), the phase is flat over the whole effective spectral region. This result indicates that the double-grating Offner stretcher is an excellent candidate in a low material-dispersion system, for example, an OPCPA system. The total transmission efficiency of the compressor was measured to be 67%. Therefore, an output energy of 3.52 J can be obtained for the compressed pulse, implying a potential peak power of 263 TW. In the next step, the full energy will be injected into the compressor after the amplified signal beam is upcollimated to 75 mm in diameter, which can ensure the output below a safe energy fluence of about 0.1 J/cm^2. Besides, the chromatic expanders will be used to replace the current expanders to optimize the space-time characterization after the compressor, which are essential for an ultrabroadband laser system to increase the actual focal-spot intensity [26]. At present, the crystal growth technology makes it possible to obtain an LBO crystal with size ~200 mm [23]. Therefore, it could support an output energy above 200 J. Considering the pulse duration of sub-15 fs, we believe it is possible to achieve a peak power over 10 PW based on LBO.

The temporal contrast is a key parameter for the application of ultraintense lasers. The temporal contrast after the third OPCPA amplifier was measured using a commercial third-order cross-correlator (Amplitude Technologies, Sequoia), as shown in Figure 7. Here, the temporal contrast shows the characteristics of prepulses free in the picosecond region, which is not easy in many high-power CPA laser systems [2, 27]. The picosecond prepulses caused by multireflections on crystal surfaces have been a well-known problem [28, 29]. In our OPCPA laser system, crystals with wedge angle of 0.5 deg were used in all the three-stage OPCPA to avoid surface reflection. The photodiode measurement also showed that no ns prepulse was detected at a dynamic range of ~10^{10}. The rising pedestal within the -100 ps time window would be originated from the far-field spectral phase noise [30–33], which can be improved by using a high-quality optical element [33] or using a stretcher based on two concave mirrors [34]. The ~10^{11} background is believed to be caused by parametric fluorescence, which could be further suppressed by adding a ps-OPA stage before the stretcher and using spatial filters between the OPCPA stages.

4. Conclusion

In conclusion, we had demonstrated the performance of the OPCPA front end for the 100 PW-level laser facility. We successfully verified two aims in the OPCPA front end: the ultrabroadband amplification to ensure >200 nm spectral

width and ultrabroadband dispersion compensation to obtain sub-15 fs compressed pulse. Using 3-stage LBO-based OPCPA, the pulse energy was boosted to 5.26 J at the repetition rate of 0.1 Hz, while the full spectral width covered 210 nm, which was limited by the bandwidth of the pulse stretcher. Without extra dispersion compensation, the pulse was compressed to 13.4 fs. Therefore, the OPCPA front end could potentially support a 263 TW peak power. To the best of our knowledge, among all the reported 100 TW-level OPCPA systems, it shows the widest spectral width, the shortest pulse duration, and it is also the first OPCPA system working at a repetition-rate mode. In the near future, with further improvement in temporal-spatial quality and operating stability, this OPCPA front end will serve as an important part of the SEL-100 PW facility.

Data Availability

The data that support the plots within this paper will be available from the corresponding authors upon reasonable request.

Conflicts of Interest

The authors declare that there is no conflict of interest regarding the publication of this article.

Acknowledgments

This work is funded by the National Key R&D Program of China (2017YFE0123700); The Strategic Priority Research Program of the Chinese Academy of Sciences (XDB1603); National Natural Science Foundation of China (61925507); Program of Shanghai Academic/Technology Research Leader (18XD1404200); Shanghai Municipal Science and Technology Major Project (2017SHZDZX02); Shanghai Sailing Program (19YF1453100); Natural Science Foundation of Shanghai (20ZR1464600); Youth Innovation Promotion Association of the Chinese Academy of Sciences; and International Partnership Program of Chinese Academy of Sciences (181231KYSB20200040).

References

[1] D. Strickland and G. Mourou, "Compression of amplified chirped optical pulses," *Optics Communications*, vol. 55, no. 6, pp. 447–449, 1985.

[2] J. H. Sung, H. W. Lee, J. Y. Yoo et al., "4.2 PW, 20 fs Ti:sapphire laser at 0.1 Hz," *Optics Letters*, vol. 42, no. 11, p. 2058, 2017.

[3] W. Li, Z. Gan, L. Yu et al., "339 J high-energy Ti:sapphire chirped-pulse amplifier for 10 PW laser facility," *Optics Letters*, vol. 43, no. 22, p. 5681, 2018.

[4] F. Lureau, G. Matras, O. Chalus et al., "High-energy hybrid femtosecond laser system demonstrating 2 × 10 PW capability," *High Power Laser Science and Engineering*, vol. 8, article e43, 2020.

[5] K. Ning, Y. Liu, J. Ma et al., "Growth and characterization of large-scale Ti:sapphire crystal using heat exchange method for ultra-fast ultra-high-power lasers," *CrystEngComm*, vol. 17, no. 14, pp. 2801–2805, 2015.

[6] S. Laux, F. Lureau, C. Radier et al., "Suppression of parasitic lasing in high energy, high repetition rate Ti:sapphire laser amplifiers," *Optics Letters*, vol. 37, no. 11, pp. 1913–1915, 2012.

[7] Y. Chu, X. Liang, L. Yu, L. Xu, R. Li, and Z. Xu, "Theoretical model to suppress parasitic lasing in large-aperture Ti:sapphire amplifiers using a temporal dual-pulse pump," *Optics Communications*, vol. 318, pp. 67–73, 2014.

[8] A. Dubietis, G. Jonušauskas, and A. Piskarskas, "Powerful femtosecond pulse generation by chirped and stretched pulse parametric amplification in BBO crystal," *Optics Communications*, vol. 88, no. 4-6, pp. 437–440, 1992.

[9] X. Zeng, K. Zhou, Y. Zuo et al., "Multi-petawatt laser facility fully based on optical parametric chirped-pulse amplification," *Optics Letters*, vol. 42, no. 10, pp. 2014–2017, 2017.

[10] X. Cai, X. Lin, G. Li, J. Lu, Z. Hu, and G. Zheng, "Rapid growth and properties of large-aperture 98%-deuterated DKDP crystals," *High Power Laser Science and Engineering*, vol. 7, article e46, 2019.

[11] A. Lyachev, O. Chekhlov, J. Collier et al., "The 10PW OPCPA Vulcan Laser Upgrade," in *Advances in Optical Materials*, OSA Technical Digest (CD) (Optica Publishing Group), 2011.

[12] J. Bromage, S. W. Bahk, I. A. Begishev et al., "Technology Development for Ultraintense All-OPCPA Systems," *High Power Laser Science and Engineering*, vol. 7, p. e4, 2019.

[13] J. Bromage, S. W. Bahk, I. A. Begishev et al., "MTW-OPAL—a technology development platform for ultra-intense all-OPCPA systems," in *2021 Conference on Lasers and Electro-Optics (CLEO)*, pp. 1-2, San Jose, CA, USA, 2021.

[14] J. Kawanaka, K. Tsubakimoto, H. Yoshida et al., "Conceptual design of sub-exa-watt system by using optical parametric chirped pulse amplification," *Journal of Physics: Conference Series*, vol. 688, article 012044, 2016.

[15] I. B. Mukhin, A. A. Soloviev, E. A. Perevezentsev et al., "Design of the front-end system for a subexawatt laser of the XCELS facility," *Quantum Electronics*, vol. 51, no. 9, pp. 759–767, 2021.

[16] V. V. Lozhkarev, G. I. Freidman, V. N. Ginzburg et al., "Compact 0.56 petawatt laser system based on optical parametric chirped pulse amplification in KD∗ P crystals," *Laser Physics Letters*, vol. 4, no. 6, p. 421, 2007.

[17] E. Cartlidge, "Eastern Europe's laser centers will debut without a star," *Science*, vol. 355, no. 6327, p. 785, 2017.

[18] Y. Wu, L. Ji, and R. Li, "On the upper limit of laser intensity attainable in nonideal vacuum," *Photonics Research*, vol. 9, no. 4, p. 541, 2021.

[19] C. N. Danson, C. Haefner, J. Bromage et al., "Petawatt and exawatt class lasers worldwide," *High Power Laser Science and Engineering*, vol. 7, article e54, 2019.

[20] Y. Peng, Y. Xu, and L. Yu, "Overview and status of station of extreme light toward 100 PW," *Reza Kenkyu*, vol. 49, pp. 93–96, 2021.

[21] F. Wu, X. Liu, X. Wang et al., "Use of double-grating Offner stretcher for dispersion control in petawatt level optical parametric chirped pulse amplification systems," *Optics & Laser Technology*, vol. 148, article 107791, 2022.

[22] J. Wang, H. Yu, Y. Wu, and R. Boughton, "Recent developments in functional crystals in China," *Engineering*, vol. 1, no. 2, pp. 192–210, 2015.

[23] H. Tu, Z. Hu, Y. Zhao, Y. Yue, J. Hou, and F. Fan, "Growth of large aperture LBO crystal applied in high power OPCPA schemes," *Journal of Crystal Growth*, vol. 546, article 125728, 2020.

[24] B. Shao, Y. Li, Y. Peng et al., "Broad-bandwidth high-temporal-contrast carrier-envelope-phase-stabilized laser seed for 100 PW lasers," *Optics Letters*, vol. 45, no. 8, pp. 2215–2218, 2020.

[25] Y. Huang, L. Song, D. Wang et al., "High-temporal-quality injector generated by optical parametric amplification with hollow-core-fiber compression," *Optics Letters*, vol. 36, no. 24, pp. 4785–4787, 2011.

[26] G. Pariente, V. Gallet, A. Borot, O. Gobert, and F. Quéré, "Space-time characterization of ultra-intense femtosecond laser beams," *Nature Photonics*, vol. 10, no. 8, pp. 547–553, 2016.

[27] Z. Zhang, F. Wu, J. Hu et al., "The 1PW/0.1 Hz laser beamline in SULF facility," *High Power Laser Science and Engineering*, vol. 8, 2020.

[28] J. Wang, P. Yuan, J. Ma, Y. Wang, G. Xie, and L. Qian, "Surface-reflection-initiated pulse-contrast degradation in an optical parametric chirped-pulse amplifier," *Optics Express*, vol. 21, no. 13, pp. 15580–15594, 2013.

[29] X. Wang, X. Lu, X. Guo, R. Xu, and Y. Leng, "Experimental investigation on pulse-contrast degradation caused by surface reflection in optical parametric chirped-pulse amplification," *Chinese Optics Letters*, vol. 16, no. 5, article 053201, 2018.

[30] J. Bromage, C. Dorrer, and R. K. Jungquist, "Temporal contrast degradation at the focus of ultrafast pulses from high-frequency spectral phase modulation," *Journal of the Optical Society of America B*, vol. 29, no. 5, p. 1125, 2012.

[31] J. Ma, P. Yuan, J. Wang et al., "Spatiotemporal noise characterization for chirped-pulse amplification systems," *Nature Communications*, vol. 6, no. 1, p. 6192, 2015.

[32] X. Lu, X. Wang, Y. Leng et al., "Suppressing temporal pedestal in Nd:glass laser systems by avoiding far-field spectral phase noise," *IEEE Journal of Selected Topics in Quantum Electronics*, vol. 24, no. 5, 2018.

[33] L. Ranc, C. Le Blanc, N. Lebas et al., "Improvement in the temporal contrast in the tens of ps range of the multi-PW Apollon laser front-end," *Optics Letters*, vol. 45, no. 16, pp. 4599–4602, 2020.

[34] X. Lu, H. Zhang, J. Li, and Y. Leng, "Reducing temporal pedestal in a Ti:sapphire chirped-pulse amplification system by using a stretcher based on two concave mirrors," *Optics Letters*, vol. 46, no. 21, pp. 5320–5323, 2021.